JOURNAL OF MATERIALS SCIENCE 22 (1987) 3265–3275

The thermal reactions of montmorillonite studied by high-resolution solid-state ^{29}Si and ^{27}Al NMR

I. W. M. BROWN, K. J. D. MacKENZIE, R. H. MEINHOLD
Chemistry Division, DSIR, Private Bag, Petone, New Zealand

Only very slight changes are observed in the ^{29}Si and ^{27}Al solid-sate magic-angle spinning NMR spectra of a montmorillonite containing almost equal numbers of octahedral aluminium and magnesium ions when its interlayer water is driven off by heating. The ^{29}Si NMR spectra are unaffected by dehydroxylation which begins at $\sim 450°$ C, but the ^{27}Al spectra show a decrease in total intensity, possibly due to the formation of 5-coordinated aluminium, with a slight increase in the intensity of the tetrahedral aluminium resonance. On the basis of these results, a structural model is proposed for the dehydroxylate phase and its formation mechanism is discussed. The destruction of the dehydroxylate X-ray pattern at $\sim 850°$ C and the subsequent recrystallization of the high-temperature products (β-quartz, enstatite and high-cordierite at $\sim 1100°$ C; β-cristobalite, enstatite and sapphirine at $\sim 1200°$ C) is accompanied by changes in the silicon and aluminium NMR spectra and in the ^{57}Fe Mössbauer spectra which are fully consistent with the known structural features of these phases.

1. Introduction

Montmorillonite, a member of the smectite group of clay minerals, is a 2 : 1 layer-lattice silicate with swelling properties derived from the presence of variable amounts of interlayer water (or other species). Structurally, montmorillonite is related to pyrophyllite, $Al_4Si_8O_{20}(OH)_4$ with varying degrees of substitution of octahedral magnesium for aluminium, charge balance being achieved by the presence of interlayer cations such as Ca^{2+} or Na^+. The general formula is therefore $(Al, Mg, Fe)_4(Si, Al)_8O_{20}(OH)_4(\frac{1}{2}Ca, Na)_{0.7} \cdot nH_2O$. On heating, the interlayer water is driven off at 110 to 140° C, accompanied by a contraction of the basal spacing from 1.5 to ~ 1.0 nm. Most of the hydroxyl water is lost at ~ 500 to 700° C [1], with the formation of a dehydroxylate phase (called an anhydride in the earlier literature). The diffuse X-ray pattern of montmorillonite survives dehydroxylation, but is abruptly lost at ~ 850 to 950° C, the exact temperature depending on the chemical composition [2]. In samples with a high degree of magnesium substitution (sometimes called Cheto-type [2]), recrystallization of β-quartz and cordierite ($Al_3Mg_2Si_5AlO_{18}$) follows almost immediately, with β-cristobalite appearing at higher temperatures, whereas in the more aluminous samples (sometimes called Wyoming-type [2]), the recrystallization of mullite and cristobalite may be delayed for a further 200 to 250° C after the loss of structure [2].

The outstanding problems in understanding the structure changes accompanying the thermal reaction sequence arise from the diffuse X-ray patterns of both the starting material and the dehydroxylate, which militate against a precise X-ray structure determination. In the 2 : 1 layer silicates, three types of octahedral sites can be distinguished, two of which are associated with hydroxyls in a *cis*-configuration (sometimes called the M2 sites), the third site being associated with *trans*-hydroxyls (the M1 sites). The earliest suggested montmorillonite structure, by Hoffmann *et al.* [3], assumed the hydroxyls to be in *trans* positions with respect to the octahedral ions (Fig. 1a), analogous to the accepted pyrophyllite structure of the time. By contrast with pyrophyllite, further refinement of the montmorillonite structure by X-ray methods has not been possible; an alternative structure postulated by Edelman and Favejee [4] was not based on direct evidence.

In attempting to deduce a structure for the dehydroxylate, Bradley and Grim [5] assumed a montmorillonite structure with only the *cis*-octahedral sites occupied (Fig. 1b); such a structure had not previously been considered, but in introducing it without comment as to its origin, Bradley and Grim may have mistaken it for the generally accepted Hoffman structure.

The most recent advances in montmorillonite structure elucidation result from oblique-texture electron diffraction studies such as those of Tsipursky and Drits [6], who worked with samples saturated with potassium to improve their structural ordering. In the 20 dioctahedral smectites studied, these workers found considerable variation in the cation distribution over the available octahedral sites; in some samples, one *trans* and one *cis* site is occupied (Fig. 1a), resembling Hoffman's structure, while in other samples, only the *cis* sites are occupied (Fig. 1b), resembling Bradley and Grim's structure. The latter structure, which has

0022–2461/87 $03.00 + .12

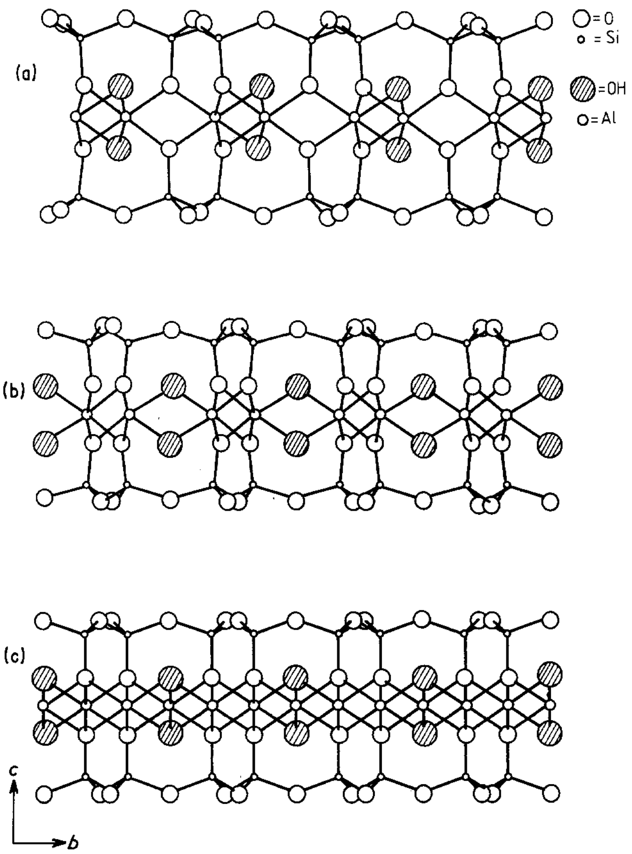

Figure 1 Computer-generated views along the *a*-axis of various structural models previously proposed for montmorillonite, based on structural data of Tsipursky and Drits [6]. (a) one *cis* and one *trans* octahedral site occupied, corresponding to the structure of Hofmann *et al.* [3]. (b) Only the *cis* octahedral sites occupied, corresponding to the concept of Bradley and Grim [5]. (c) All the available octahedral sites randomly occupied with equal probability.

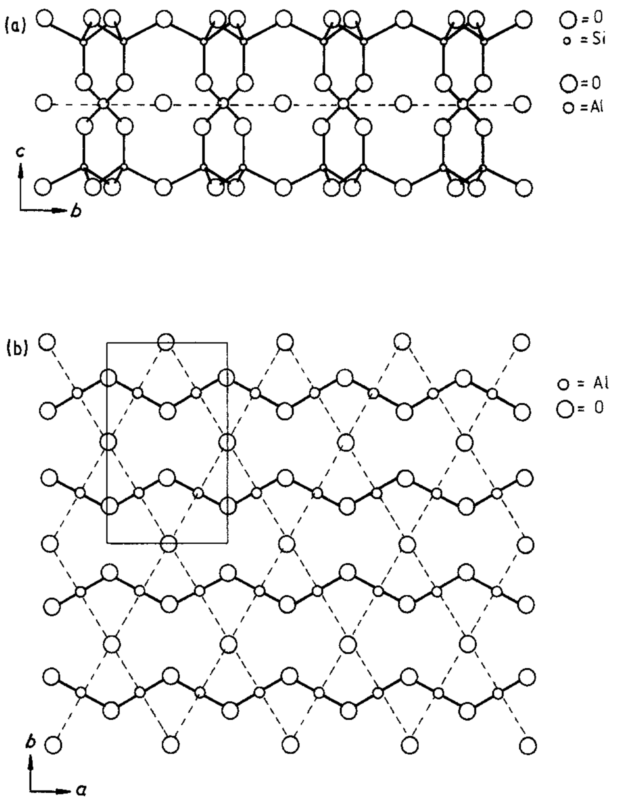

Figure 2 Computer-generated structure of montmorillonite dehydroxylate, after Bradley and Grim [5]. Broken lines indicate metal–oxygen bonds postulated by Bradley and Grim, but too long to be within practical bonding distance. (a) View along the *a*-axis; (b) projection on the 0 0 1 plane (silicon-containing tetrahedral layers omitted for clarity).

no centre of symmetry, is generally adopted by nontronites (iron-rich smectites). A third possibility has also been recognised [6] in which all the available octahedral sites are randomly occupied with equal probability (Fig. 1c). The structural type which will be adopted cannot readily be predicted from the chemical composition of the octahedral layers [6].

These uncertainties about the montmorillonite structure were perpetuated in the speculations regarding the dehydroxylate, for which only one formalized structure has been proposed [5]. This assumes a starting material with only one of the *cis* sites occupied (Fig. 1b) and its formation involves the shifting of the residual hydroxyl oxygens into the *c*-axis plane of the octahedral ions, which themselves undergo significant displacement in the *b*-axis. As visualized by Bradley and Grim [5] and later discussed by Johns and Jonas [7], the resulting aluminium configuration is formally 6-coordinate, although with two improbably long M–O bonds (0.26 nm), making it effectively square-planar (Fig. 2). Computer simulation of this structure shows the shorter Al–O bond lengths to be 0.1725 nm (mean) and the mean tetrahedral O–Si–O angles 118.9°.

The Bradley and Grim dehydroxylate model is both structurally implausible and is inconsistent with the result of an IR study by Heller *et al.* [8] which ruled out 4-coordinate (square-planar) aluminium in montmorillonite dehydroxylate. However, the IR results were not inconsistent with 5-coordinate aluminium, as was subsequently found in pyrophyllite dehydroxylate [9, 10] (although the IR spectra indicated that the initial structures of montmorillonite and pyrophyllite are less analogous than had previously been assumed).

In an attempt to shed light on the structure of the dehydroxylate, Heller-Kallai and Rozenson [11] have studied the changes in the environment of the octahedral iron by Mössbauer spectroscopy. On the expectation that cations in the M1 (*trans*-OH) sites remain 6-coordinate on dehydroxylation, whereas the M2 (*cis*-OH) cations become 5-coordinate, these authors have resolved their Mössbauer spectra into two doublets with quadrupole splittings (QS) of 1.78 to 1.80 and 1.16 to 1.31 mm sec^{-1}, assigning these to 6-coordinate and 5-coordinate Fe^{3+}, respectively.

However, the general philosophy of assigning pairs of fitted doublets to specific sites in smectites has been questioned by Cardile and Johnston [13] who suggest that these two-doublet computer fits are an artefact which describes the extremes of a continuum of Fe^{3+} sites of slightly different energies; this raises doubts about the structural conclusions of the Mössbauer study of montmorillonite dehydroxylate.

The newly-developed technique of high-resolution solid-state ^{27}Al and ^{29}Si NMR with magic-angle spinning (MAS) has recently proved useful in helping to elucidate the thermally-induced structural changes in pyrophyllite (which forms a crystalline dehydroxylate [10]) and in kaolinite, which forms an X-ray amorphous

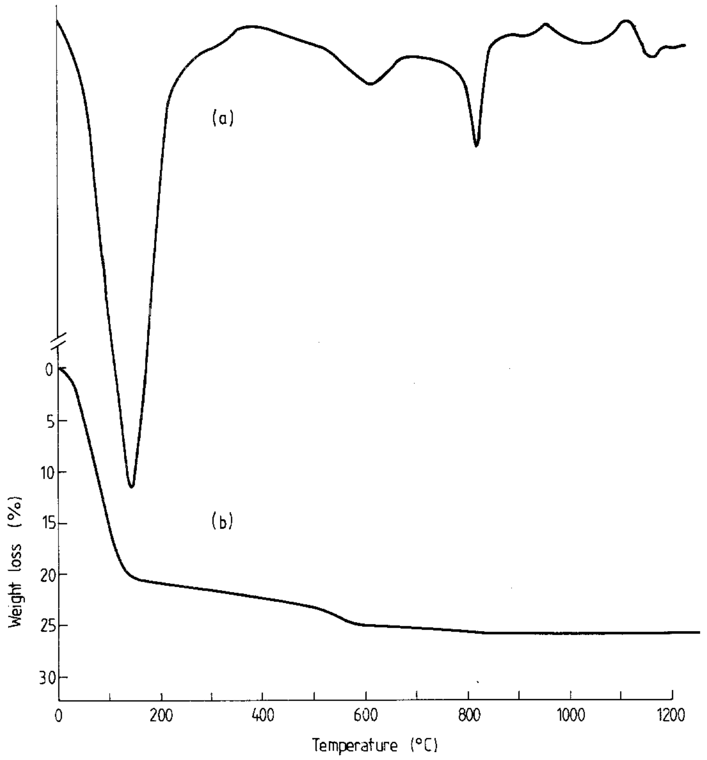

Figure 3 Thermal analysis curves for Yavapai montmorillonite, heating rate 10° C in air (min^{-1}). (a) Differential thermal analysis curve; (b) thermogravimetric curve.

dehydroxylate [14]. The thermal reaction sequence of montmorillonite was therefore subjected to a similar study, complemented by thermal analysis, X-ray diffraction and Mössbauer spectroscopy.

2. Experimental procedure

The montmorillonite studied here, from Yavapai County, Arizona, USA, was chosen because its iron content was suitably low for an NMR study, while still being sufficient for Mössbauer spectroscopy. The chemical analysis and unit cell contents, calculated by the method of Ross and Hendricks [15], are shown in Table I.

The X-ray diffraction pattern showed only the characteristic broad reflections of montmorillonite, with a basal spacing of ~ 1.5 nm. Thermogravimetric analysis and DTA was carried out in static air at a heating rate of $10° \text{C} \, \text{min}^{-1}$. The solid-state MAS NMR spectra of samples heated for 15 min at various temperatures up to 1300° C were obtained using a Varian XL 200 spectrometer at magic-angle spinning speeds of 2 to 2.5 kHz. ^{29}Si spectra were obtained at 39.7 MHz with gated decoupling and a recycle delay of 0.5 sec. T_1(Si) was estimated by progressive saturation to be 0.02 sec; ^{1}H relaxation was too fast for accurate measurement. Cross-polarization spectra were obtained with a recycle delay of 0.1 sec and generally a contact time of 1 m sec due to short $T_{1\varrho}$(H). ^{27}Al spectra at 52.1 MHz were obtained with a 0.1 sec delay between pulses. A short 2 μsec (ca. $\pi/15$) pulse was used to reduce contributions from satellite transitions and enable comparison with the peak area of the α-alumina used as an external standard for determination of aluminium content.

TABLE I Chemical analysis and unit cell formula of Yavapai montmorillonite (based on 20O, 4(OH)*

Component	Content (wt %)	Unit cell formula	
SiO_2	48.16	Si 7.90	8.0
Al_2O_3	12.43	Al 0.10	
MgO	7.91		
CaO	1.12	Al 2.30	4.56
TiO_2	0.33	Mg 1.94	
Fe_2O_3	2.59	Fe^{3+} 0.32	
Na_2O	0.04		
K_2O	0.05	Ca 0.40	
H_2O^-	21.20		
H_2O^+	5.83	O 20	
Total	99.67	(OH) 4	

*Analysts: R. L. Goguel and J. G. Webster.

Chemical shifts were referenced indirectly to tetramethylsilane or $Al(H_2O)_6^{3+}$. Because of the tendency of samples heated below 350° C to rehydrate rapidly, special precautions were taken with these samples. After cooling in a desiccator they were pressed into the Kel-F rotors and sealed by pressing on a capping layer of elemental sulphur, followed by a pressed boric acid layer, to keep the sample intact during spinning. The rotor was then sealed with a piece of Teflon tape and the commercial rotor cap. The successful sealing of hygroscopic materials in this way was demonstrated with P_2O_5 samples, which showed no measurable weight gains over several hours exposure to ambient laboratory conditions.

X-ray powder diffraction was carried out on all samples using a Philips PW1050/7 diffractometer with cobalt radiation and a graphite monochromator, and the Mössbauer spectra were obtained using an Elscint AME 50 spectrometer with a Co/Rh source (Elscint Inc., Hackensack, New Jersey). All spectra were computer-fitted, and the isomer shifts are quoted with respect to natural iron.

3. Results and discussion

3.1. Thermal analysis of montmorillonite

The thermal analysis curves are shown in Fig. 3. These curves are typical of montmorillonite, the 21.2% endothermic weight loss up to 230° C being due to the removal of interlayer water, as evidenced by the concomitant collapse of the basal spacing from ~ 1.5 to 1.0 nm. Below about 450° C, this collapse was found to be reversible due to rapid rehydration on exposure to the atmosphere, but samples heated to above 450° C did not regain their 1.5 nm basal spacing on standing. The broad endothermic event at ~ 630° C corresponds with the loss of ~ 4% hydroxyl water; its broadness may be due to the presence of two overlapping peaks which are resolved in some montmorillonites [16]. Dehydroxylation produces no noticeable change in the X-ray pattern. Gradual weight loss continues up to ~ 850° C when a small, sharp endotherm occurs. This peak, which has previously been reported in Yavapai montmorillonite [16], may be characteristic of samples with high magnesium content [16], and corresponds with the formation of an X-ray amorphous phase. A suggestion by McConnell [17] that this endotherm represents the loss of excess hydroxyl water located in the *tetrahedral* layer, possibly in association with tetrahedral aluminium, is not consistent with the very small degree of aluminium-for-silicon substitution in the present material. A weak exotherm at 950° C corresponds with the appearance of β-quartz and enstatite ($MgSiO_3$), while the exotherm at 1120° C marks the conversion of β-quartz to β-cristobalite, and the appearance of a little high-cordierite ($Mg_2Al_4Si_5O_{18}$). These high-temperature phases are consistent with those reported for magnesium-rich (so-called "Cheto-type") samples [2]. At 1150° C, a previously unreported product phase, sapphirine, $(Mg, Fe)_4Al_8Si_2O_{20}$ forms at the expense of the cordierite, and by 1300° C the sample has melted.

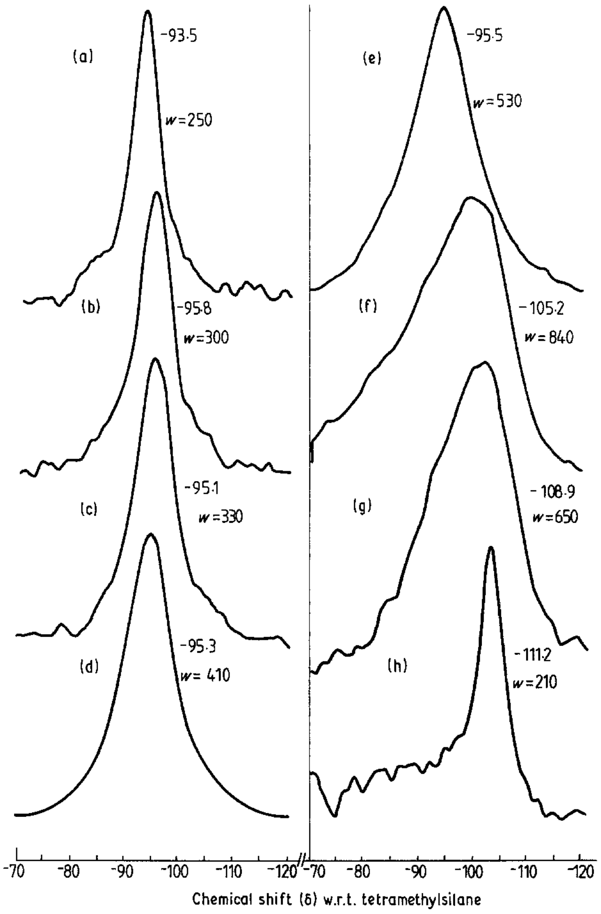

Figure 4 High-resolution solid-state ^{29}Si NMR spectra of Yavapai montmorillonite heated to the temperatures indicated for 15 min. Chemical shifts and widths at half height as indicated. (a) Unheated, (b) 140° C, (c) 250° C, (d) 480° C, (e) 640° C, (f) 850° C, (g) 1000° C, (h) 1200° C.

3.2. NMR spectroscopy

The ^{29}Si MAS NMR spectra of Yavapai montmorillonite heated to various temperatures are shown in Fig. 4. The silicon resonance of the unheated material (Fig. 4a) is almost twice the width of the peak for kaolinite determined under similar conditions [18], consistent with the poorer crystallinity of the montmorillonite giving rise to a wider range of silicon environments (alternatively the broadness of the ^{29}Si peak in montmorillonite has been ascribed to dipolar interaction with Fe^{3+} in the aluminium sites [19]). The present ^{29}Si chemical shift is in good agreement with previously reported values for natural and synthetic samples (−93 p.p.m. [20, 21] and −94.1 p.p.m. [19]).

In samples heated to below ~ 300° C, in which the loss of interlayer water appears to be reversible, a small change of ~ 2 p.p.m. is found in the ^{29}Si chemical shift, *irrespective of whether or not the sample is allowed to rehydrate*. Thus, the initial loss of interlayer water produces a slight change in the silicon environment which is not reversed by rehydration, even though the original interlayer spacing is restored. This effect appears to be associated with the interlayer cation, since the ^{29}Si chemical shift of a potassium-saturated Yavapai sample retained its initial value of −93.6 p.p.m. during dehydration and rehydration below ~ 300° C. Loss of interlayer water at increasing temperatures produces a progressive broadening of the silicon peak (Figs 4a to c), a trend which continues with hydroxyl water loss at ~ 630° C (Fig. 4e). Dehydroxylation produces no further change in the silicon chemical shift, which remains at about −95.5 p.p.m. until the structure breaks down at ~ 840° C, at which stage the chemical shift changes to −105.2 p.p.m. (Fig. 4f), and the width increases to a value similar to that of metakaolinite [18], a similarly X-ray amorphous dehydroxylated phase. Recrystallization of silica is accompanied by a narrowing of the silicon resonance line and further changes in chemical shift (Figs 4g and h) which at 1000° C approaches the value reported for quartz (−108 p.p.m. [20]) and, at 1200° C cristobalite (−110 p.p.m. [20]). The silicon spectra of samples heated at 850 and 1000° C show a pronounced assymetry, which at 1000° C has the appearance of shoulders at about −85, −95 and −100 p.p.m. (Fig. 4g). These chemical shifts are consistent with those of the secondary high-temperature phases enstatite (−81 and −83 p.p.m. [20]) and cordierite (−79 and −100 p.p.m. [22]); during the present work, ^{29}Si chemical shifts of −97 to −100.3 p.p.m. were also found for various samples of synthetic and natural high- and low-cordierite.

Previous ^{29}Si NMR studies of pyrophyllite [10] and kaolinite [14] have invoked an empirical relationship

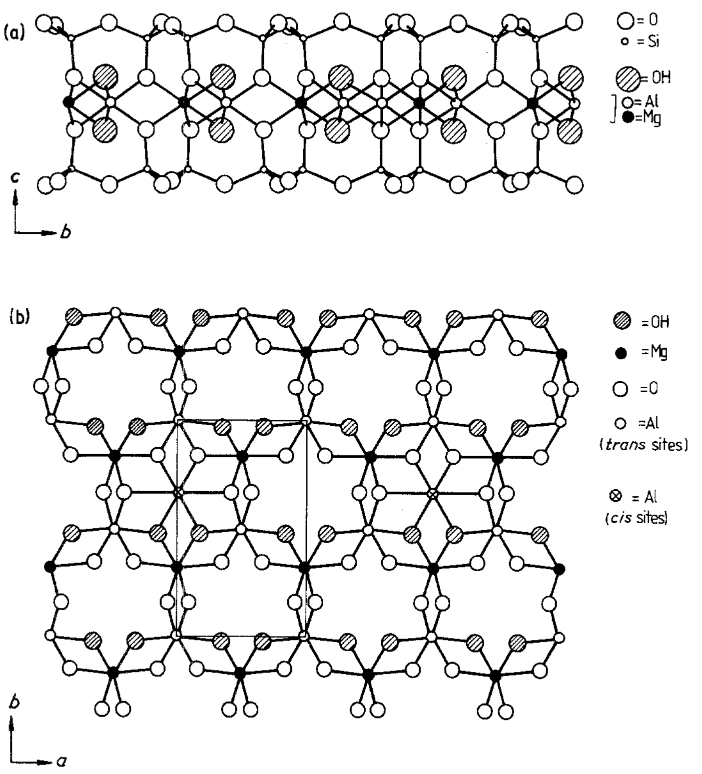

Figure 5 Computer-generated model of a representative portion of the Yavapai montmorillonite structure, based on chemical analyses and solid-state NMR data. (a) View along the *a*-axis; (b) projection on the 0 0 1 plane (tetrahedral silicon-containing layers omitted for clarity).

between the mean tetrahedral bond angle θ and the chemical shift δ:

$$\delta = -176.65 - 55.821 \sec \theta \qquad (1)$$

The relationship has been found to hold for a number of silicates and aluminosilicates including clay minerals for which good structural data are available, and it has also been used to provide information about phases of less well defined structures [10, 14]. Using a computer programme [23] to generate bond lengths and angles from the structural data for the three proposed montmorillonite models of Tsipursky and Drits [6], their Model 1 (with the two equivalent *cis*-hydroxyl sites occupied) is found to have $\theta = 130.89°$, corresponding to a calculated δ of -91.38 p.p.m. Model 2 (one *cis* and one *trans*-hydroxyl site occupied) has slightly different θ values for the two types of silicon, corresponding to calculated δ values of -90.88 and -92.24 p.p.m., respectively. Both these models give δ values within ~ 2 p.p.m. of the observed value, and are thus equally feasible for the present material. The third model (all sites randomly occupied with equal probability) gives a calculated δ of -85.73 p.p.m., and is therefore less consistent with the observed value. Computer simulation indicates that in Model 1, the occupied octahedral sites have identical Al–O distances (0.1937 nm), whereas in Model 2, the *trans*-OH sites are of smaller bond lengths than the *cis*-OH sites (0.1919 and 0.1962 nm, respectively). On the reasonable assumption that the smaller (*trans*) sites will be favoured by aluminium and the larger (*cis*) sites by magnesium, the unit cell contents of Yavapai montmorillonite (Table I) could be accommodated by Model 2 provided the excess aluminiums occupy the third (*cis*) site which is vacant in Model 2. The stoichiometry requires a 28% occupancy of the third site, which, if filled randomly, results in a structure of which part is shown in Fig. 5.

In this structure six out of eight of the silicons are in configurations having calculated δ values of -90.9 and -92.2 p.p.m., the other two out of eight silicons (associated with the additional aluminium in the third octahedral site) having calculated δ values of -83.9 to -85.7 p.p.m., depending on the degree of adjustment assumed to occur in the octahedral layer in the regions where the vacant site is filled. This model therefore predicts the spectrum of the unheated material to be broadened, with some assymetry arising from the component at about -80 to -85 p.p.m., this is a reasonably accurate description of the observed spectrum (Fig. 4a).

On dehydroxylation of the structure of Fig. 5, considerable rearrangement of the octahedral layer will occur (Fig. 6), resulting in the formation of predominantly 5-coordinated aluminium, but with smaller amounts of 4- and 6-coordinated aluminium, as discussed later. However, calculations of the silicon chemical shift from this computer-simulated dehydroxylate model predict that the silicon spectrum should be unchanged by dehydroxylation. This is consistent with the observed spectrum (Fig. 4e), which is however broadened due to increased disorder introduced by heating, or perhaps by closer approach of the Fe^{3+} sites by the ^{29}Si. By comparison, the silicon chemical shift calculated from the computer simulation of the Bradley and Grim [5] dehydroxylate model (-61.3 p.p.m.) bears no resemblance to the observed shift, underlining the unsatisfactory nature of that model. The change in the observed chemical shift accompanying the loss of X-ray structure at $\sim 840°$ C (Fig. 4f) is consistent with the separation of some of the silica from the aluminous regions, but the width and assymetry of the spectrum indicates the persistence of a wide range of silicon–aluminium environments, including some not unlike those of the original structure. Further changes in the silicon

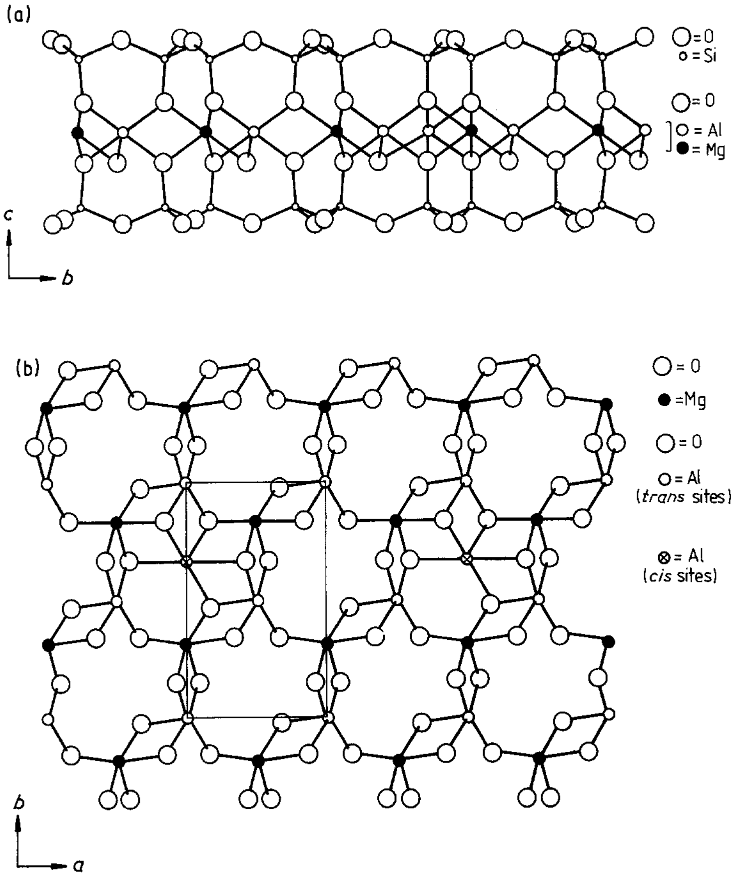

Figure 6 Computer-generated model of a representative portion of the structure of dehydroxylated Yavapai montmorillonite based on solid-state NMR data. (a) View along the *a*-axis; (b) projection on the 0 0 1 plane (tetrahedral silicon-containing layers omitted for clarity).

spectra on heating are consistent with the known spectra of the high-temperature phases identified by X-ray diffraction.

Cross-polarization (CP) measurements, made to investigate the environment of the silicon atoms in close proximity to the interlayer water and hydroxyl protons, indicate that even in the fully hydrated sample, only ~4.5% of the total silicons could be detected, possibly because of the influence of Fe^{3+} on the proton relaxation time. On removal of the interlayer water and subsequent dehydroxylation, the number of detectable CP silicons decreased further, consistent with the loss of protons from the structure (Fig. 7b). The measured δ of the CP silicon spectra remained identical to that of the non-CP spectra (Fig. 4), indicating that the chemical environments of all the silicons are similar.

The ^{27}Al NMR spectra are shown in Figure 8. As was found with other heated clay minerals [10, 14], only a small proportion of the total aluminium (in this case a maximum of ~20%) is detected by ^{27}Al NMR (Fig. 7a). As previously noted, the detectable aluminium decreases on dehydroxylation, but the detection improves slightly when the high-temperature products form (Fig. 7a). The reason why only one in five of the aluminium atoms is observed is probably related to the presence of both magnesium and Fe^{3+} in the octahedral sites. The magnesium reduces the symmetry around adjacent aluminium nuclei, increasing the electric field gradient at the nuclei. A similar effect is produced by Fe^{3+}, but in addition, the unpaired electron of the Fe^{3+} interacts with the nuclear spins of the aluminium atoms in proximity, causing their NMR signal to broaden and shift beyond detection.

The ^{27}Al spectrum of unheated montmorillonite (Fig. 8a) contains a prominent peak at 1 p.p.m. indicating that most of the detectable aluminium atoms are in octahedral sites. The smaller peaks are spinning sidebands; at present spinning speeds the sideband at 52 p.p.m. appears in the region in which tetrahedral aluminium resonances occur. Goodman and Stucki [24] have taken the presence of a small shoulder on their sideband peak at 60 to 70 p.p.m. to indicate the presence of a small amount of tetrahedral aluminium in a montmorillonite of similar composition to the present sample, but we have not considered their technique of quantification of peak ratios to be justified in the present case.

On heating Yavapai montmorillonite, little change occurs in the ^{27}Al spectra until dehydroxylation, when the proportion of tetrahedral aluminium increases (Fig. 8e), with an overall decrease in the amount of aluminium detected (Fig. 7a). This trend continues when the structure collapses (Fig. 8f), but the formation of the high-temperature phases is accompanied by an increase in the proportion of octahedral aluminium (Fig. 8h). The ^{27}Al spectra of synthetic high-cordierite and natural low-cordierite, obtained under the same conditions, bore little resemblance to the 1200° C spectrum, containing very distorted (probably 6-coordinate) sites. This suggests that in montmorillonite heated at 1200° C, the aluminium is located predominantly in the sapphirine phase; although no ^{27}Al NMR spectrum of sapphirine has been reported, its crystal structure [25, 26] contains both tetrahedral and octahedral aluminium, consistent with the ^{27}Al NMR spectrum (Fig. 8h).

By analogy with the previous NMR results for

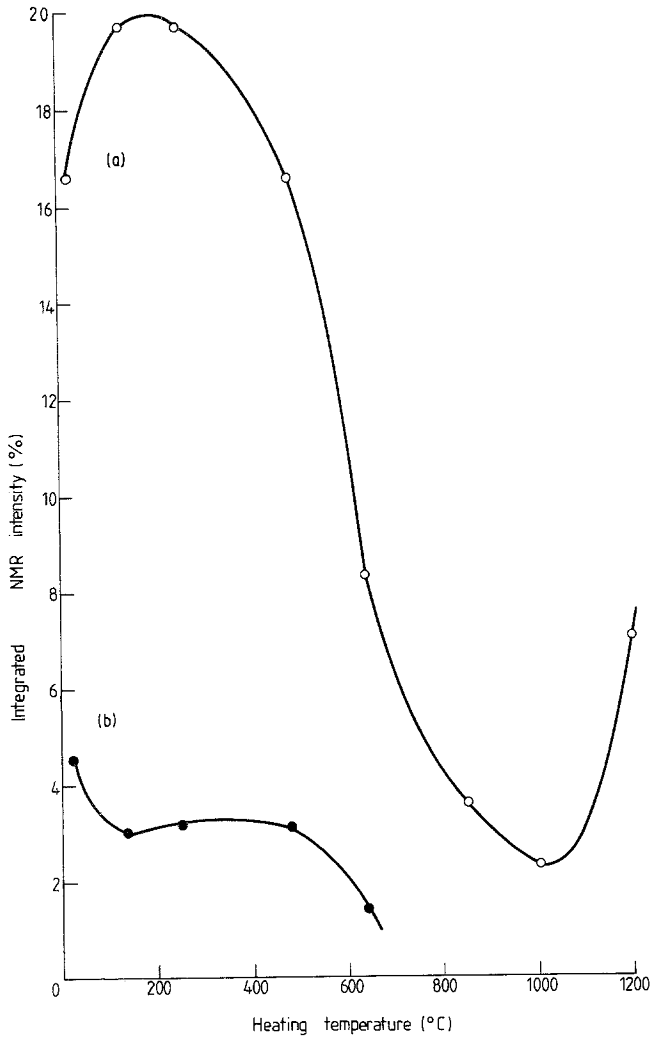

Figure 7 Change in (a) percentage of the total aluminium content observed by ^{27}Al NMR, and (b) the intensity of the cross-polarized ^{29}Si resonance as a percentage of total silicon, as a function of heating temperature.

pyrophyllite [10], the loss of aluminium signal on dehydroxylation may be understood in terms of the formation of 5-coordinate aluminium, as is predicted for all three structural models (Fig. 1), including the structure proposed for Yavapai montmorillonite (Fig 5), which takes into account the actual stoichiometry of the octahedral layer. However, the orderly elimination of pairs of hydroxyls from this structure, leaving one residual oxygen atom per pair, can proceed in two ways as illustrated in Fig. 9.

Alternate elimination of the hydroxyls marked X and Y (Path A) leads to double columns of 5-coordinate metal atoms (marked c) interspersed with alternatively 4 and 6-coordinated atoms (marked a and b, respectively). Elimination of all the X hydroxyls (or all the Y hydroxyls) by Path B (Fig. 9) leads to the formation of only 5-coordinated metal atoms. The appearance of some 4 and 6-coordinate aluminium in the ^{27}Al NMR dehydroxylate spectrum indicates that at least some of the hydroxyls are eliminated by Path A. Furthermore, of the three basic models which describe montmorillonite structures [6] (Fig. 1), only Model 2 of Tsipursky and Drits (which also coincides with Hoffmann's 1933 structure, Fig. 1a) can eliminate hydroxyls to produce 4- and 6-coordinated metal atoms, in addition to 5-coordinated ones. Thus, the present montmorillonite structure, based on Tsipursky and Drits' Model 2, is the only one which is consistent with both the ^{29}Si and ^{27}Al spectra at all temperatures.

According to the scheme of Fig. 9, complete dehydroxylation will result in the formation of both 5-coordinated aluminium and magnesium. In the present high-magnesium sample such a situation should be inherently unstable, leading to immediate structural breakdown, as in talc. However, the thermal analysis results (Fig. 3) indicate that gradual loss of a further ~ 1% water continues beyond initial dehydroxylation at ~ 600° C until structural breakdown at 840° C, suggesting that, as with pyrophyllite [10], montmorillonite dehydroxylate is not fully anhydrous. If, as seems likely, the residual hydroxyls are associated with the magnesium (*cis*) sites, a reasonable explanation is provided for their persistence to higher temperatures and the loss of structure accompanying their complete removal.

3.3. Mössbauer spectroscopy

Typical Mössbauer spectra of unheated and heated Yavapai montmorillonite samples are shown in Fig. 10. For a satisfactory computer fit of the unheated spectrum (Fig. 10a), two doublets had to be included. The parameters of the major doublet A (QS = 0.54, IS = 0.35 mm sec^{-1}) are in excellent agreement with those previously reported for Yavapai montmorillonite and assigned to Fe^{3+} in the *trans*-octahedral sites [13]. The present structural modelling (Fig. 5) suggests however that in addition to the *trans*-sites, some *cis*-sites are also occupied by aluminium, and

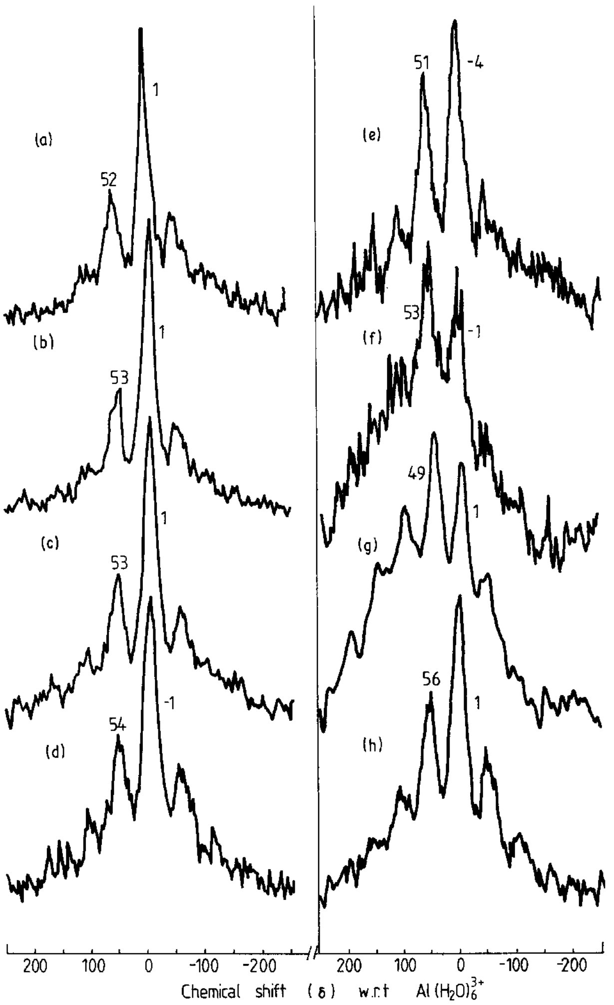

Figure 8 High-resolution solid-state ^{27}Al NMR spectra of Yavapai montmorillonite heated to different temperatures for 15 min. (a) Unheated, (b) 140° C, (c) 250° C, (d) 480° C, (e) 640° C, (f) 850° C, (g) 1000° C, (h) 1200° C.

may therefore also be substituted by Fe^{3+}. The broad, shallow minor doublet B has parameters which are difficult to define, militating against its assignment to a specific type of site. As previously suggested [13], the two doublets may represent the extremes of a range of slightly different Fe^{3+} resonances. No attempt was made to include a tetrahedral Fe^{3+} doublet, in view of the absence of significant tetrahedral aluminium substitution (and therefore tetrahedral Fe^{3+}) in the present sample.

Removal of the interlayer water by heating to 250° C produces no change in the Mössbauer spectra, which are also similar to those of heated samples which have been allowed to rehydrate. However, after heating to 480° C (at which temperature the samples do not rehydrate on standing), two further doublets, C and D (Fig. 10b) appear, at the expense of A and B. The new doublets, which are characteristic of the dehydroxylate, constitute a more sensitive indicator of the onset of dehydroxylation than solid-state NMR, which registers significant changes only at the point of structural breakdown. On heating to 640° C (Fig. 10c), the dehydroxylate doublets C and D develop further, their parameters comparing well with those reported previously for montmorillonite dehydroxylate [11], in which the wider doublet was assigned to Fe^{3+} in very distorted 6-coordinated M1 (originally *trans*) sites, the narrower doublet being ascribed to 5-coordinate Fe^{3+} in the M2 (originally *cis*) sites [11]. The present structural modelling and NMR results suggest the presence of 4-, 5-, and 6-coordinated aluminium sites into which Fe^{3+} may substitute, but the identification of these sites with Mössbauer doublets poses problems, particularly in the case of 5-coordinate Fe^{3+}, for which widely different parameters have been reported

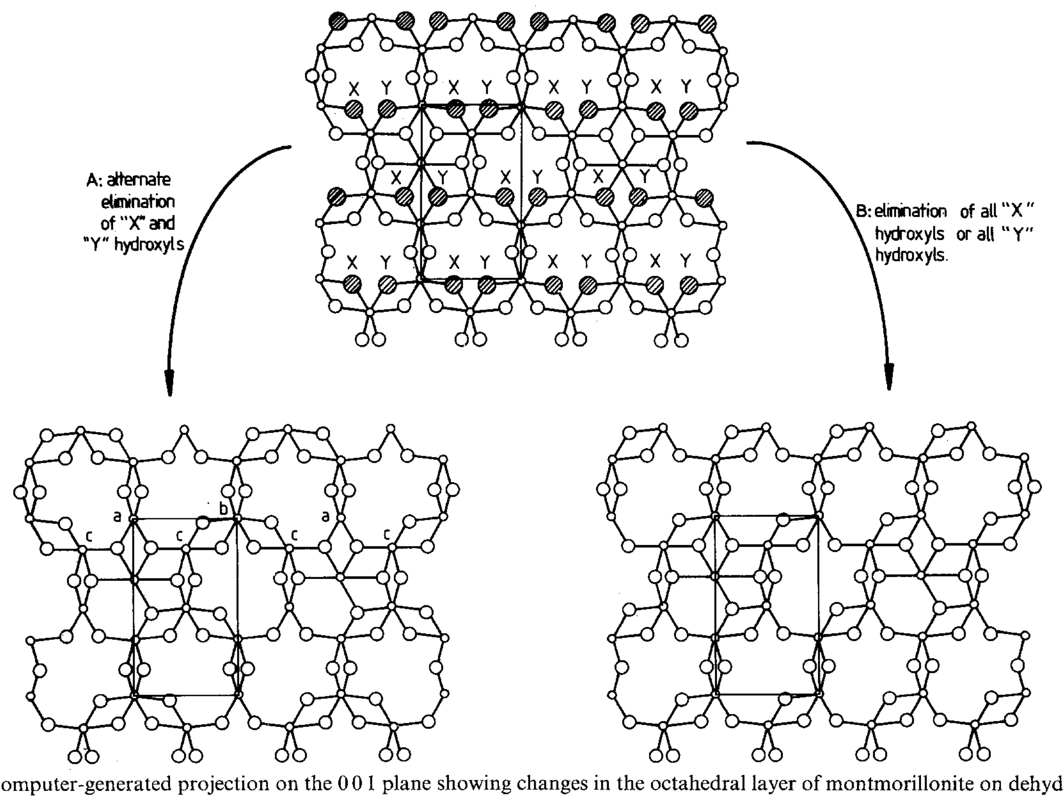

Figure 9 Computer-generated projection on the 0 0 1 plane showing changes in the octahedral layer of montmorillonite on dehydroxylation, and indicating the mechanism by which 4-, 5- and 6-coordinated metal atoms may be produced (tetrahedral silicon-containing layers omitted for clarity).

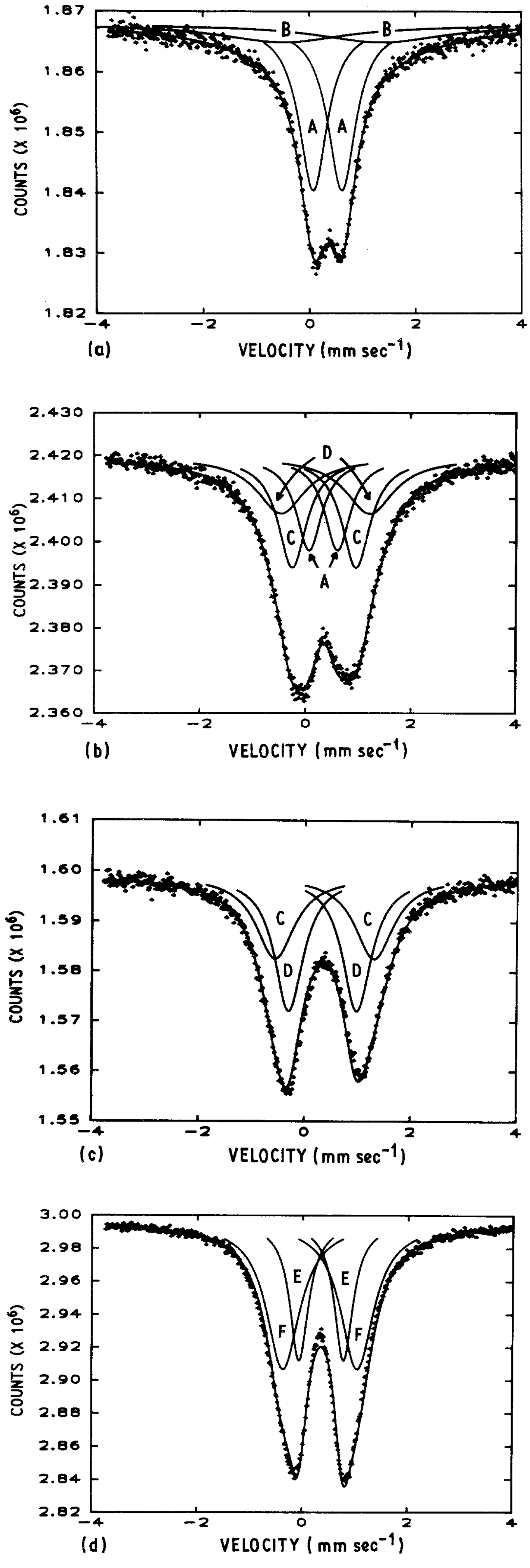

Figure 10 Typical Mössbauer spectra of Yavapai montmorillonite heated to different temperatures. (a) 25 to 250° C, (b) 480° C, (c) 640° C, (d) 850° C, (e) 1000 to 1200° C.

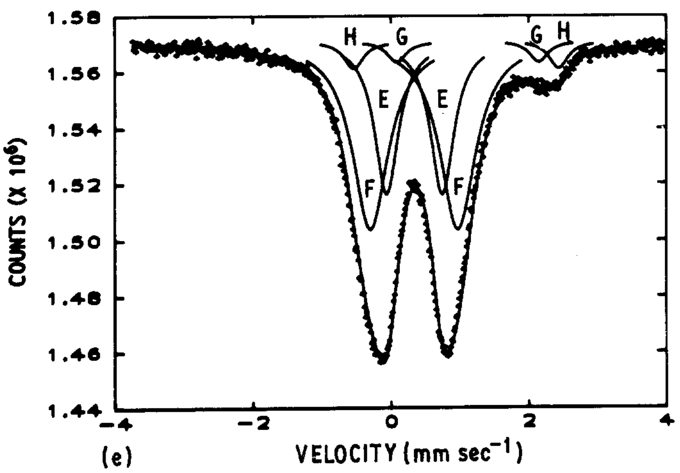

Figure 10 Continued.

($QS = 1.2$, $IS = 0.12\,mm\,sec^{-1}$ in andalusite [27] and $QS = 2.0\,mm\,sec^{-1}$ in $BaFe_{12}O_{19}$, which however has a 6-line spectrum [28].

Since the present modelling studies suggest that the largest number of sites are 5-coordinated, these may be identified with resonance D (Fig. 11), in agreement with Heller-Kallai and Rozenson [11]. Attempts to include a 4-coordinate doublet in the dehydroxylate spectra were unconvincing, since the presence of such doublets did nothing to improve the fit. The disappearance of the dehydroxylate X-ray pattern at about 850° C is accompanied by a narrowing of the Fe^{3+} linewidths, consistent with the incipient recrystallization of product phases, and the appearance of a low-intensity Fe^{2+} resonance (Fig. 10e). The changes in site occupancy during heating are summarized in Fig. 11.

By 1200° C, the parameters of the Fe^{3+} doublets E and F ($QS = 0.81$, $IS = 0.34$ and $QS = 1.35$, $IS = 0.30\,mm\,sec^{-1}$) agree well with those previously reported both for a yellow ferric sapphine ($QS = 0.78$, $IS = 0.31$ and $QS = 1.37$, $IS = 0.28\,mm\,sec^{-1}$ [29]) and for sapphine formed by thermal decomposition of the Al–Mg layer silicate amesite ($QS = 0.81$, $IS = 0.29$ and $QS = 1.36$, $IS = 0.31\,mm\,sec^{-1}$ [30]), suggesting that the Fe^{3+} resides solely in the sapphine phase.

Although the small amount of Fe^{2+} could be accommodated either in enstatite or cordierite, the latter ceases to be a significant phase at higher temperatures. The reported Mössbauer parameters of Fe^{2+} in the M1 sites of enstatite ($QS = 2.95$ to 3.18, $IS = 1.21$ to $1.26\,mm\,sec^{-1}$ [31]) compare reasonably well with those of doublet H, whereas the parameters of doublet G are comparable with those reported for the M2 sites ($QS = 2.18$ to 2.26, $IS = 1.21$ to $1.26\,mm\,sec^{-1}$ [31, 32]). The growth of doublet G at the expense of H (Fig. 11) is consistent with improved cation ordering into the more favoured M2 site [32].

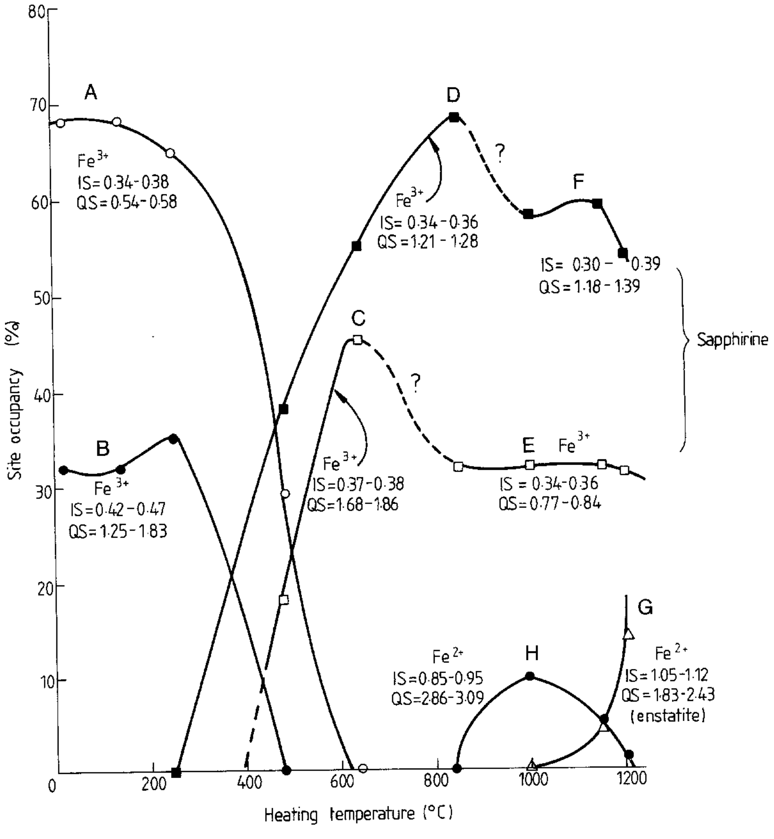

Figure 11 Changes in relative site occupancy by iron atoms in Yavapai montmorillonite as a function of heating temperature, based on computer-fitted spectral areas and assuming the recoil-free fractions of Fe^{3+} and Fe^{2+} to be approximately equal. Isomer shift values quoted with respect to natural iron. Resonances labelled as in Fig. 10.

4. Conclusions

1. Montmorillonite from Yavapai County, Arizona, containing almost equal numbers of octahedral aluminium and magnesium ions, reversibly loses its interlayer water when heated below about 450° C. This water loss is accompanied by a collapse of the X-ray basal spacing from ~ 1.5 to ~ 1.0 nm and by a change of ~ 2 p.p.m. in the ^{29}Si NMR signal. The ^{27}Al spectrum is unchanged by the interlayer water loss. On exposure to laboratory air, the samples rehydrate, regaining their original basal spacing, but not the original ^{29}Si chemical shift.

2. With the onset of dehydroxylation at about 450° C, the basal spacing is not regained on standing, but the X-ray pattern and silicon and aluminium NMR spectra are otherwise largely unchanged. A more senstive indicator of dehydroxylation is the Mössbauer spectrum of the Fe^{3+} substitutional impurity atoms, which in the dehydroxylate can be resolved into two doublets tentatively assigned to 5-coordinated and distorted 6-coordinated sites. Even when dehydroxylation is essentially complete at 640° C, the ^{29}Si spectrum, although broadened, retains its chemical shift of -95.5 p.p.m. but the amount of aluminium detectable by NMR decreases to $\sim 4\%$ of the total aluminium content, possibly due to the formation of 5-coordinated aluminium.

3. Computer modelling studies of the various possible structures of the starting material and dehydroxylate indicate that the elimination of hydroxyl groups from Yavapai montmorillonite can give rise both to 5-coordinated aluminium, and to smaller amounts of 4- and 6-coordinated aluminium, fully consistent with all the NMR results.

4. A further gradual water loss precedes the destruction of the dehydroxylate structure at 850° C. ^{29}Si and ^{27}Al NMR indicates that the resulting X-ray-amorphous phase contains silicon in a wide range of environments, but the aluminium-containing regions retain elements of the dehydroxylate structure. The crystalline products which appear at higher temperatures reflect the chemical constitution of the starting material; at 1100° C, β-quartz recrystallizes with the separation of enstatite ($MgSiO_3$) containing a small amount of substitutional Fe^{2+}. The aluminium is initially accommodated in a high-cordierite phase ($Mg_2Al_2Si_5O_{18}$) which at higher temperatures is replaced by sapphirine, $(Mg, Fe)_4Al_8Si_2O_{20}$, containing the remainder of the impurity iron as substitutional Fe^{3+}. By 1200° C, the β-quartz has completely transformed β-cristobalite. The ^{29}Si, ^{27}Al and Mössbauer spectra are fully consistent with these high-temperature transformations.

Acknowledgements

We are indebted to Mr R. M. Berezowski for technical assistance.

References

1. R. E. GRIM and W. F. BRADLEY, *J. Amer. Ceram. Soc.* **23** (1940) 242.
2. R. E. GRIM and G. KULBICKI, *Amer. Mineral.* **46** (1961) 1329.
3. U. HOFMANN, K. ENDELL and D. WILM, *Z. Krist.* **86** (1933) 340.
4. C. H. EDELMAN and J. Ch. L. FAVEJEE, *ibid.* **102** (1940) 417.
5. W. F. BRADLEY and R. E. GRIM, *Amer. Mineral.* **36** (1951) 182.
6. S. I. TSIPURSKY and V. A. DRITS, *Clay Min.* **19** (1984) 177.
7. W. D. JOHNS and E. C. JONAS, *J. Geol.* **62** (1954) 163.
8. L. HELLER, V. C. FARMER, R. C. MacKENZIE, B. D. MITCHELL and H. F. W. TAYLOR, *Clay Min. Bull.* **5** (1962) 56.
9. R. WARDLE and G. W. BRINDLEY, *Amer. Mineral.* **57** (1972) 732.
10. K. J. D. MacKENZIE, I. W. M. BROWN, R. H. MEINHOLD and M. E. BOWDEN, *J. Amer. Ceram. Soc.* **68** (1985) 266.
11. L. HELLER-KALLAI and I. ROZENSON, *Clays Clay Mins* **28** (1980) 355.
12. I. ROZENSON and L. HELLER-KALLAI, *ibid.* **28** (1980) 391.
13. C. M. CARDILE and J. H. JOHNSTON, *ibid.* **34** (1986) 307.
14. K. J. D. MacKENZIE, I. W. M. BROWN, R. H. MEINHOLD and M. E. BOWDEN, *J. Amer. Ceram. Soc.* **68** (1985) 293.
15. C. S. ROSS and S. B. HENDRICKS, US Geological Survey Professional Paper 205-B (1945) 23-79.
16. R. GREENE-KELLY, in "The Differential Thermal Investigation of Clays", edited by R. C. MacKenzie (Mineralogical Society, London, 1957) pp. 140–64.
17. D . McCONNELL, *Amer. Mineral.* **35** (1950) 166.
18. R. H. MEINHOLD, K. J. D. MacKENZIE and I. W. M. BROWN, *J. Mater. Sci. Lett.* **4** (1985) 163.
19. T. WATANABE, H. SHIMIZU, A. MASUDA and H. SAITO, *Chem. Lett.* (1983) 1293.
20. K. A. SMITH, R. J. KIRKPATRICK, E. OLDFIELD and D. M. HENDERSON, *Amer. Mineral.* **68** (1983) 1206.
21. J. G. THOMPSON, *Clay Min.* **19** (1984) 229.
22. A. PUTNIS, C. A. FYFE and G. C. GOBBI, *Phys. Chem. Minerals* **12** (1985) 211.
23. S. MOTHERWELL, "PLUTO, A Programme for Plotting Molecular and Crystal Structures" (University Chemical Library, Cambridge, England, 1976).
24. B. A. GOODMAN and J. W. STUCKI, *Clay Min.* **19** (1984) 663.
25. P. B. MOORE, *Amer. Mineral.* **54** (1969) 31.
26. S. MERLINO, *Z. Krist.* **151** (1980) 91.
27. U. HALENIUS, *Can. Mineral.* **16** (1978) 567.
28. E. KREBER, U. GONSER, A. TRAUTWEIN and F. E. HARRIS, *J. Phys. Chem. Solids* **36** (1975) 263.
29. G. M. BANCROFT, R. G. BURNS and A. J. STONE, *Geochim. Cosmochim. Acta* **32** (1968) 547.
30. K. J. D. MacKENZIE and M. E. BOWDEN, *Thermochim. Acta* **64** (1983) 83.
31. T. V. MALYSHEVA and A. V. UKHANOV, *Geochem. Int.* **13** (1976) 96.
32. R. G. GUPTA and R. G. MENDIRATTA, *Mineralog. Mag.* **43** (1980) 815.

Received 20 October 1986
and accepted 22 January 1987